Fabrication and Characterization of Porous Silicon for Photonic Applications

**Arvin I. Mabilangan*, Niel Gabriel E. Saplagio,
Eloise P. Anguluan, Neil Irvin F. Cabello,
Rhona Olivia M. Gonzales, Armando S. Somintac
and Arnel A. Salvador**
University of the Philippines Diliman

ABSTRACT

Porous silicon (PSi) thin films from p-type silicon (100) substrates were fabricated using a simple table top electrochemical etching setup with a 1:1 HF:EtOh electrolyte solution. Porous silicon films with different morphologies and optical properties were achieved by varying the etching parameters, such as HF concentration, etching time and anodization current. It was observed that the film thickness of the fabricated PSi increased with etch time and HF concentration. The etch rate increased with the applied anodization current. Reflection spectroscopy at normal incidence was used to determine the refractive indices of the fabricated films. Using the Sellmeier equation, the chromatic dispersion of the films was obtained for different HF concentrations and anodization currents.

Keywords: Silicon, anodization, porous materials, photonic applications

INTRODUCTION

Porous silicon is a two-phase composite material with a refractive index that can vary from air to silicon (Si). Porous silicon, among other porous materials, is non-toxic and is relatively more affordable to produce because of the abundance of silicon. Porous silicon has been shown to produce photoluminescence despite its base material's indirect bandgap (Canham 1990), which paved the way for applications in optoelectronics (Bisi and others 2000). Its high surface-to-volume ratio and high reactivity to chemicals makes it a good candidate for gas (Naderi and others 2012) and chemical sensors (Ozdemir and others 2010). Furthermore, its absorbance has

_____
*Corresponding author

made it a suitable material for photodetectors (Garcia and others 2008) and solar cell devices (Ramizy and others 2011). Aside from the abundance of silicon, the simplicity of its fabrication and its variable refractive index due to its controllable porosity make it possible to create components or materials for photonic applications without the use of vacuum chambers and expensive deposition techniques. These applications include wave guides (Jelenski and others 2005), dichroic mirrors (Diener and others 2001), rugate filters (Lorenzo and others 2005), and Fabry-Perot filters (Vinegoni and others 2000).

The structure of porous silicon is dependent on the HF concentration, current density, etch rate, substrate doping, type of electrolyte solution, and type of electrochemical cell (Halimaoui and others 1995), among other parameters. The exact process of formation is not yet clear; however, there are many proposed models as to how it is

Hole injection and attack on a Si-H bond by fluoride ion

Second attack by a fluoride ion with hydrogen evolution and electron injection into the substrate

HF attack the Si-Si backbonds. The remaining Si surface atoms are bonded to the H atoms and a silicon tetrafluoride (SiF_4) molecule is produced.
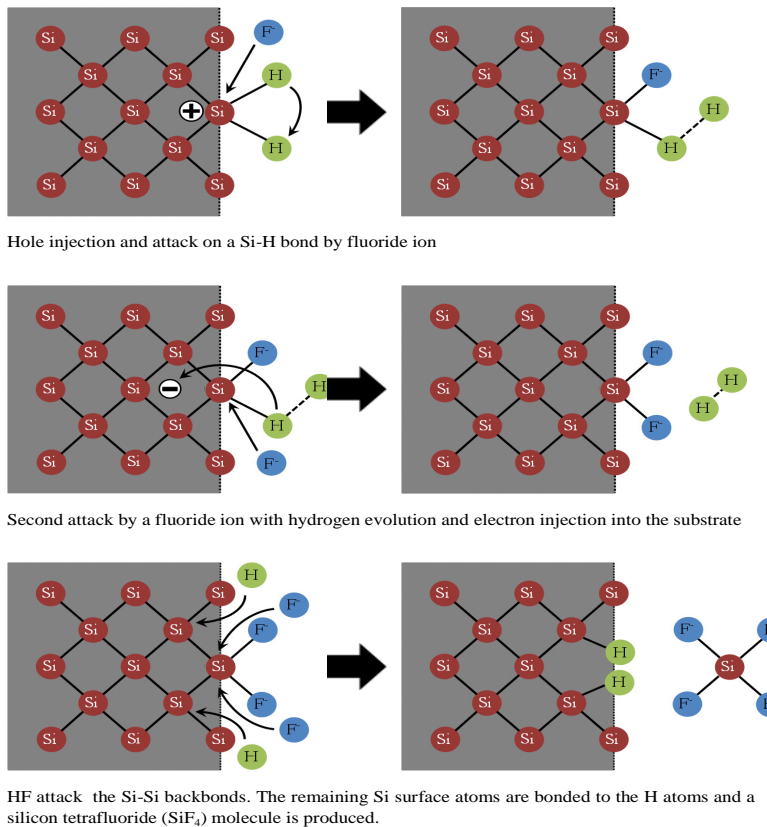
Figure 1. Mechanism of the electrochemical dissolution of Si in an HF based electrolyte proposed by Gösele and Lehmann. Adapted from O. Bisi and others (2000).

formed. The model of Gösele and Lehmann (1991) posits that electronic holes present on the surface of silicon cause the fluorine ions (F^-) to attack the silicon hydride (Si-H) bonds, forming hydrogen gas and SiF_4 & H_2SiF_6 which are dissolved in the solution. The etched silicon loses the holes in the process preventing further reaction with the F^- ions (see Figure 1).

In this work, PSi was fabricated from p-type (100) silicon by means of a simple tabletop electrochemical etching setup. Etching parameters such as HF concentration, etch time and current were varied to characterize their effect on the thickness and refractive index of the PSi. These results are important in further exploration of PSi for photonic applications.
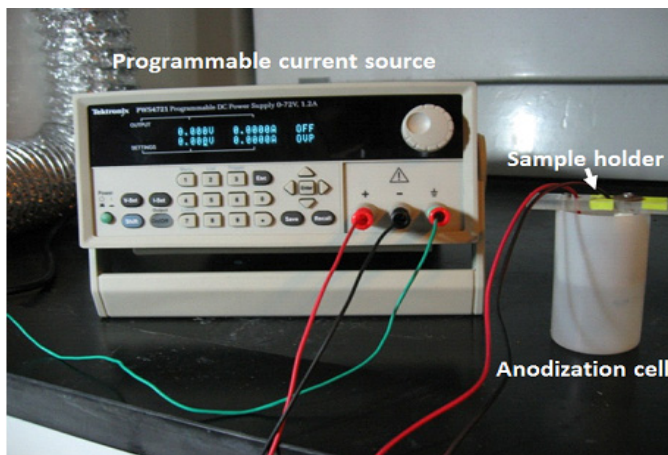
(a)
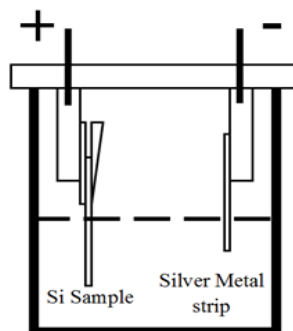
(b)

Figure 2. Actual setup (a) and schematic diagram of the anodization cell (b) of the electrochemical etching setup used in fabricating PSi films.

METHODOLOGY

The substrate used was a 500μm thick, polished on one side, monocrystalline p-type silicon wafer with (100) orientation cut into 1x1.5cm samples. The silicon substrates were subjected to standard degreasing procedures and the unpolished surface was covered with an HF-resistant polymer before electrochemical etching. The electrochemical etching was done using a simple tabletop setup shown in Figure 2. The sample was attached to a plexiglass sample holder with a silver metal cathode and the silicon sample as the anode. The sample holder was lowered into the single tank anodization cell so that 1x1cm of the silicon was submerged into a 1:1 solution of hydrofluoric acid (HF) and absolute ethanol. A Tektronix PWS4721 programmable current source was used to drive the electrochemical process in the system. After etching, the samples were rinsed with absolute ethanol to reduce surface tension between the pores.

HF concentrations were varied (6%, 9%, 12%, and 24%), as well as the current supplied (1mA, 5mA, 10mA, 15mA, and 20mA) and etch times (from 3mins to 20mins). Each parameter was varied while keeping the other two constant to establish the effects of each on the morphology of the fabricated PSi and the corresponding effect on its optical properties.

A Philips XL 30 FEG Scanning Electron Microscopy (SEM) was used to determine the thickness and pore dimensions of the PSi. Reflectance Spectroscopy was also used to determine the wavelength-dependent refractive index of the samples through a Sellmeier equation fit. The reflectivity of the samples was characterized in the range 400-1100nm.

RESULTS AND DISCUSSION

Photonic materials greatly depend on the physical dimension and refractive index of the material used. The variability of the morphology such as thickness and porosity of PSi is essential.
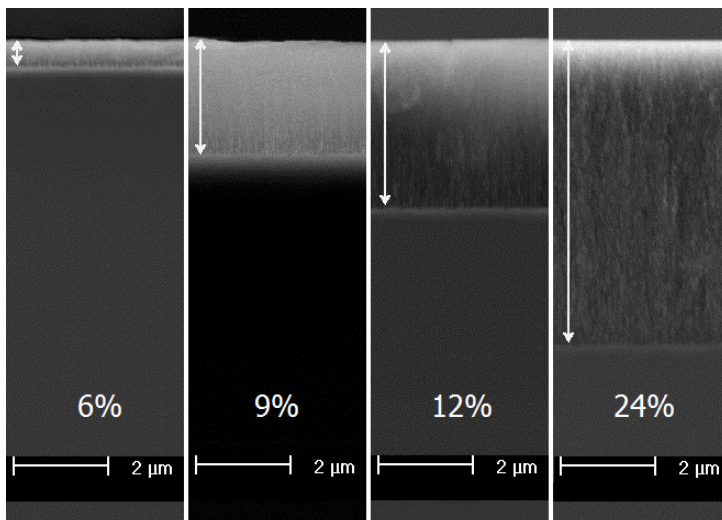
PSi Film Thickness

Figure 3 shows the dependence of film thickness on the HF concentration used in the electrolyte. The increasing trend means that the production of PSi is faster for higher HF concentrations. This can be attributed to the abundance of F^- ions that attack the Si-H bonds in the electrolyte. The increase in the F^- ion population in the etching solution lessens the time between reactions, thus hastening the etching and producing PSi much faster. From the trend, we can predict that for concentrations

lower than 5%, PSi formation may not be possible because the applied anodic current may not be sufficient to drive the etching reaction through the resistive solution.
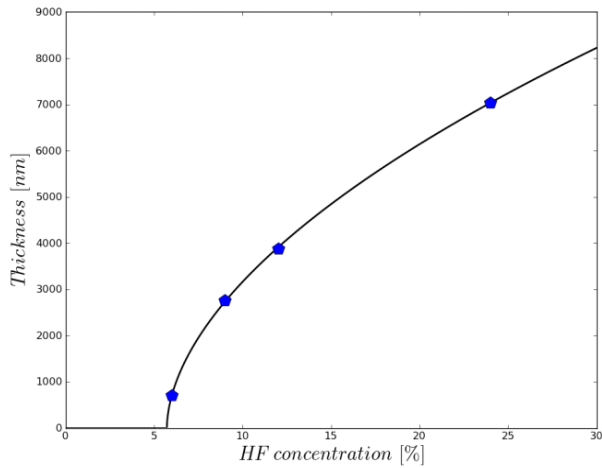

(a)

(b)

Figure 3. Thickness dependence of PSi films on HF concentration (a) and their corresponding cross sectional SEM micrographs (b). All PSi films are etched at 10mA for 10mins.

Figure 4 shows the thickness variation of the PSi films etched at different times for two different anodization currents. For both PSi etched at 5mA and 15mA, it was observed that as the etching time was increased, the thickness of the PSi film also increased but at different rates. The thickness of the films fabricated with
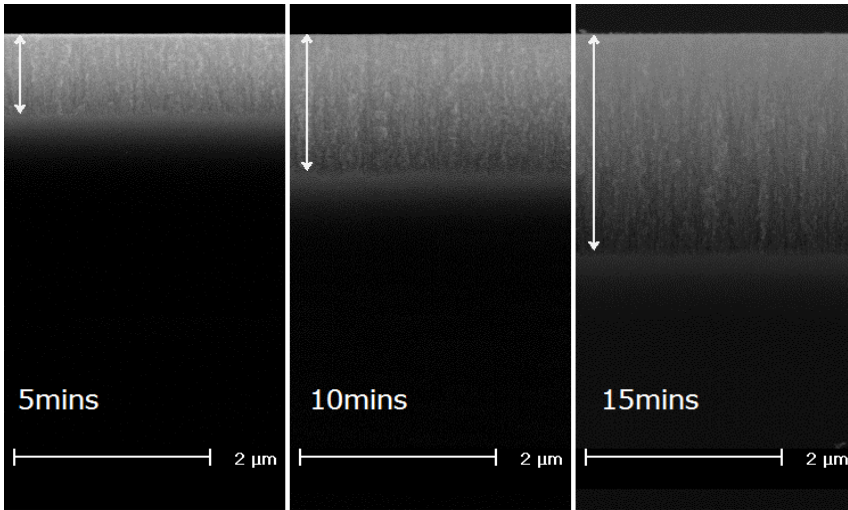

(a)
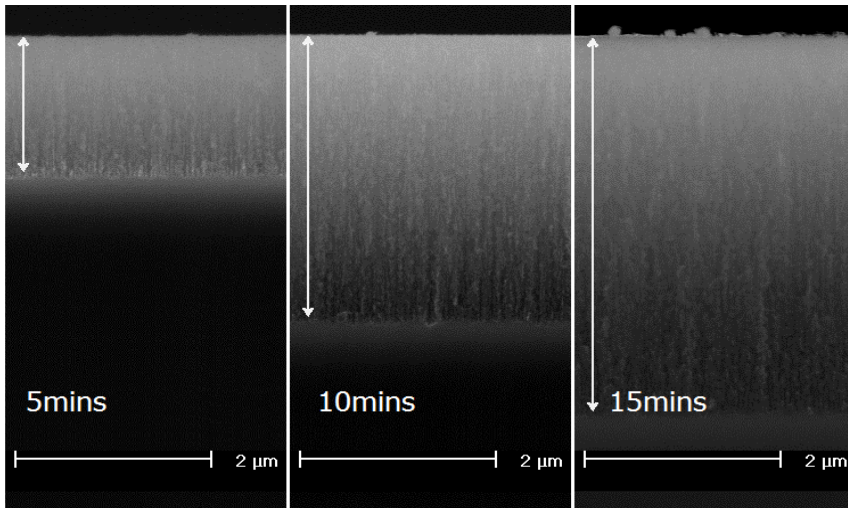
(b)

Figure 4. Cross-sectional SEM micrographs of PSi etch at 5mA (a) and 15mA (b) for different etching times. All PSi was etched with 12% HF concentration.

varying etch time and anodization current was plotted (Figure 5a) and the etch rate was calculated. For each anodization current, the thickness depends linearly with the etch time. The etch rate, however, depends non-linearly with the anodization current (Figure 5b). The obtained results agree with the results of Berger and others (1997).
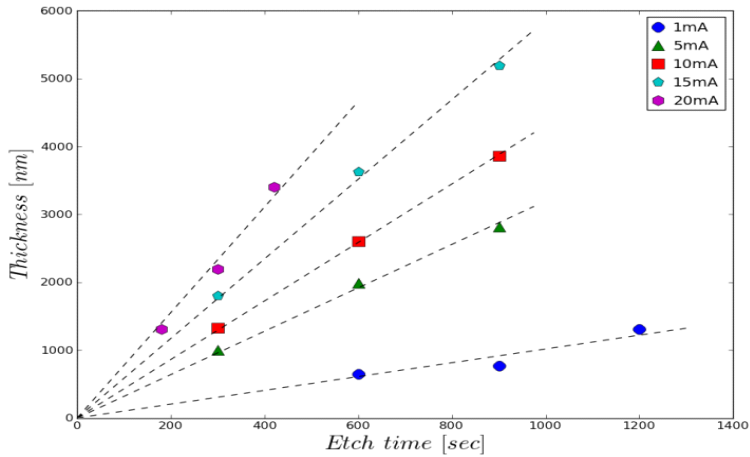
(a)
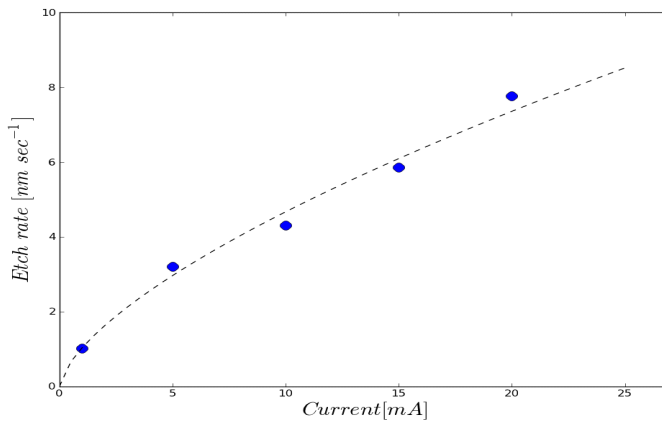
(b)

Figure 5. Thickness dependence of fabricated PSi films on etching time for different anodization currents (a); Etch rate vs. anodization current density (b).

21

Pore Size and Refractive Index

Being able to tune the refractive index of porous silicon is one of its most important characteristics in order for it to act as a waveguide. The results obtained show that the refractive index of porous silicon can be tuned by changing one or more of its etching parameters to effectively vary the pore size.

The observed increase in pore size as the HF concentration decreases (Figure 6) is due to the favored chemical etching (lateral) rather than electrochemical etching (vertical) because of the consequent increase in the resistivity of the solution. Therefore, lower refractive index is expected for PSi etched at lower HF concentrations because of the decrease in optical density (higher air-to-silicon ratio because of larger pore size). The refractive indices of PSi films were obtained using reflectance spectroscopy at normal incidence. Using the local minima and maxima observed in each reflectivity spectrum, we can compute the refractive indices through

$$n = \frac{i\lambda_0\lambda_i}{2d(\lambda_i - \lambda_0)} \tag{1}$$

where i is the number of complete cycles between two local minima or maxima (λ_0 and λ_i) and d is the film thickness (Schroder 2006). The reflectivity spectra for films with small d are expected to have fewer oscillations over the chosen scan range of 400-1100 nm, and thus less computed n values.

From the calculated refractive indices, a Sellmeier fit (2) is used to obtain the wavelength-dependent refractive index or dispersion curve of the samples,

$$n^2(\lambda) = 1 + \frac{A\lambda^2}{\lambda^2 - B^2} + \frac{C\lambda^2}{\lambda^2 - D^2} \tag{2}$$

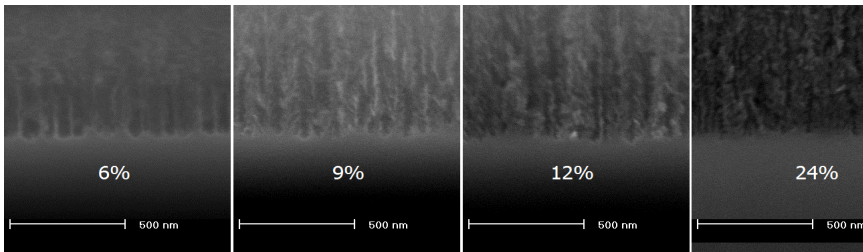where A, B, C, and D are fitting parameters.

Figure 6. Pore size dependence of PSi etched for different HF concentration. All PSi films are etched at 10mA for 15mins.

Since PSi is considered a two-phase composite material of air and silicon, we expect that its refractive index varies between air and silicon (1.00 to 3.44). We can describe the quantity of air and silicon in the PSi by the porosity, formally defined as the volumetric ratio between the air in the pores and the bulk silicon before it was etched. However, since Si exhibits wavelength-dependent refractive index or chromatic dispersion, we also expect PSi to exhibit this property. Figure 7 shows the dependence of the refractive index of porous silicon on the HF concentration used. It can be noted that higher concentrations produce higher ranges of refractive indices. This result agrees with the decrease in pore dimensions at higher concentrations as shown earlier. Since pores are much larger in less concentrated solutions, their refractive indices are expected to approach that of air; the samples etched in higher concentrations form smaller pores and are expected to have a refractive index closer to that of silicon. The figure also shows the 24%HF samples reaching up to a refractive index twice of that obtained for the 6%HF concentration, where the dispersion curves are shifted upward as concentration is increased.
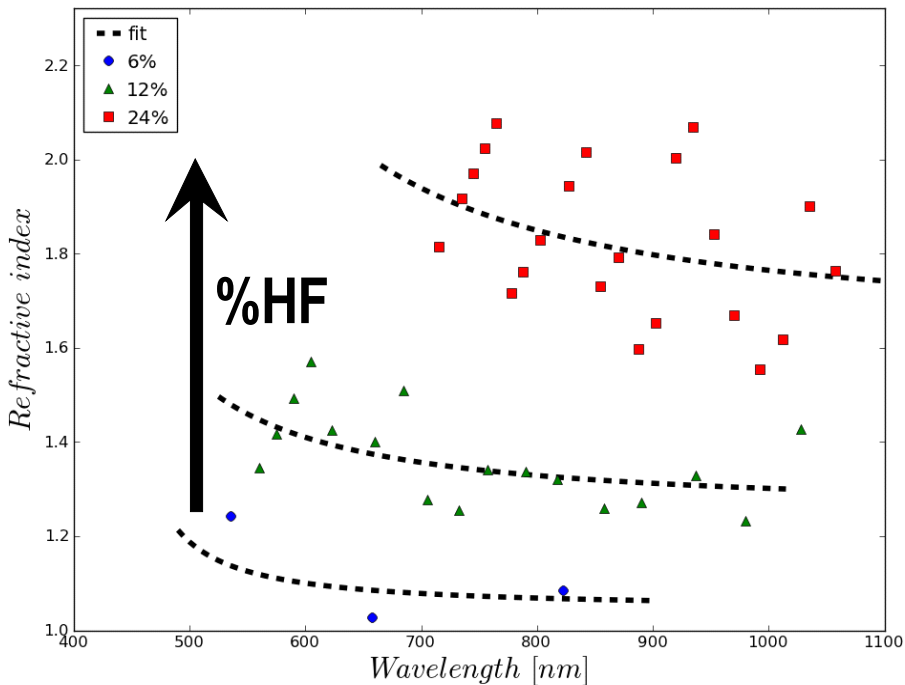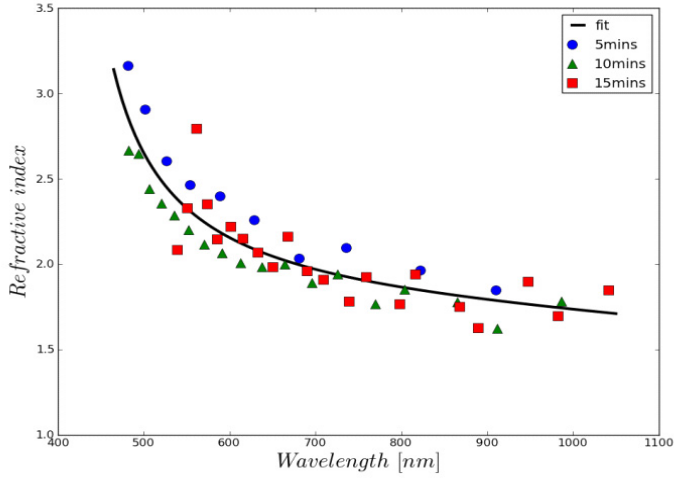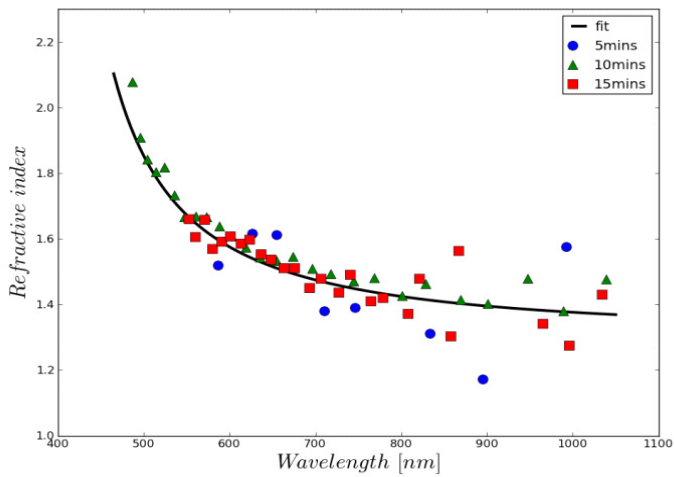

Figure 7. Computed refractive indices of PSi films fabricated at different HF concentrations. Each dot represents the refractive index *n* computed from equation (1) for each of the 3 samples, fabricated at 10mA for 15mins using different HF concentrations (6%, 12%, 24%).

Figure 8 shows the computed refractive indices for different etch times. The computed refractive indices for varying etch times follow roughly the same dispersion curves for both 5mA and 15mA anodization currents (Figure 8). This result supports the assumption that as etch time is increased, the porosity of the sample remains fairly constant. The pore size is unaffected by longer etch times.

(a)

(b)

Figure 8. Computed refractive indices of PSi films fabricated at 5mA (a) and 15mA (b) for different etching times in a 12% HF solution.

Figure 9 shows the fitted dispersion curves for different anodization currents. The refractive index was observed to decrease as current density increased due to the increase in porosity of the PSi layer. This agrees with the result regarding the pore dimensions as discussed earlier.

When higher anodization currents are used, an increase in the electron hole population in the Si surface occurs. As a result, sites for pore formation are increased, thereby increasing the average number of pores. This, in effect, increases the ratio of air-to-silicon of the sample, which translates to the lower refractive indices for higher current densities used.
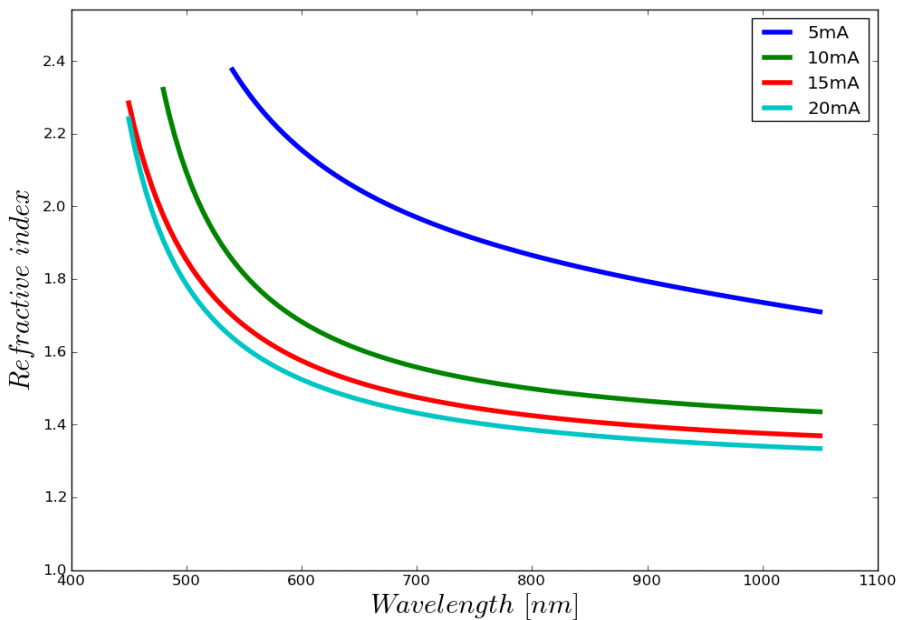

Figure 9. Chromatic dispersions obtained through Sellmeier equation for PSi etched at different anodization currents.

SUMMARY

Porous silicon was successfully fabricated from p-type silicon (100) substrates using a simple tabletop electrochemical etching setup with HF as the electrolyte. Fabrication parameters such as HF concentration, etch time, and anodization current were varied to establish a relationship with these parameters to the thickness and refractive index of porous silicon.

PSi film thickness increases for longer etch times and higher HF concentrations. Constant etch rates have been observed for different anodization currents. Etch rates follow a nonlinear increase as the anodization current is increased. The refractive index of the fabricated PSi depends on the pore size, which is dependent only on the HF concentration and anodization current. Lower HF concentration produces larger pore sizes that decrease the refractive index due to higher air-to-silicon ratio, producing lower dispersion curves. PSi fabrication with high anodization currents tends to have lower dispersion curves due to the increase in the sites for pore formation.

Photonic devices such as distributed Bragg reflectors and photonic crystals can thus be made from porous silicon using a simple electochemical etching setup due to the ease in controlling film thickness and refractive index.

ACKNOWLEDGMENTS

REFERENCES

Badoz PA, Bensahel D, Bomchil G, Ferrieu F, Halimaoui A, Perret P, Regolini J, Sagnes I, Vincent G. 1992. Characterization of porous silicon: Structural, optical and electrical properties. Mat. Res. Soc. Symp. Proc. 283: 97-108.

Berger MG, Arens-Fisher R, Thonissen M, Kruger M, Billat S, Luth H, Hilbrich S, Thiess W, Grosse P. 1997. Dielectric filters made of PS: Advanced performance by oxidation and new layer structures. Thin Solid Films 297(1-2): 237-240.

Bisi O, Ossicini S, Pavesi L. 2000. Porous silicon: A quantum sponge structure for silicon based optoelectronics. Surf. Sci. Rep. 38: 1-126.

Canham LT. 1990. Silicon quantum wire array fabrication by electrochemical and chemical dissolution of wafers. App. Phys. Lett. 57(10): 1046-1048.

Diener J, Künzner N, Kovalev D, Gross E, Yu V, Timoshenko, Polisski G, Koch F. 2001. Dichroic Bragg reflectors based on birefringent porous silicon. App. Phys. Lett. 78: 3887-3889.

Gösele U, Lehmann V. 1991. Porous silicon formation: A quantum wire effect. App. Phys. Lett. 58(8): 856-858.

Halimaoui A. 1997. Porous silicon formation by anodisation. In Canham, LT editor. Properties of porous silicon. London, United Kingdom. The Institution of Electrical Engineers. p 12-22.

Jeleñski AM, Gawlik G, Wesolowski M. 2005. Silicon applications in photonics. Proceedings of SPIE, Volume 5948: 59480X.

Lee Y, Lee J, Shul Y, Lim S. 2008. Effect of wafer resistivity and HF concentration on the formation of vertically aligned porous silicon. Journal of Industrial and Engineering Chemistry 14(1): 105-109.

Lorenzo E, Oton CJ, Capuj NE, Ghulinyan M, Navarro-Urrios D, Gaburro Z, Pavesi L. 2005. Porous silicon-based rugate filters. Applied Optics 44(26): 5415-5421.

Naderi N, Hashim MR, Amran TST. 2012. Enhanced physical properties of porous silicon for improved hydrogen gas sensing. Superlattices and Microstructures 51(5): 626-634.

Ozdemir S, Gole JL. 2010. A phosphine detection matrix using nanostructure modified porous silicon gas sensors. Sensors and Actuators B: Chemical 151(1): 274-280.

Ramizy A, Wisam J, Aziz Z, Hassan, Khalid Omar, Ibrahim K. 2011. Improved performance of solar cell based on porous silicon surfaces. Optik-International Journal for Light and Electron Optics 122(23): 2075-2077.

Salgado G, Hernández R, Martínez J, Díaz T, Juárez H, Rosendo E, Galeazzi R, García A, Juárez G. 2008. Fabrication, characterization, and analysis of photodetectors metal-porous silicon with different geometry and thickness of the porous silicon layer. Microelectronics Journal 39(3–4): 489-493.

Schroder DK. 2006. Optical characterization–reflection. In: Schroder DK, editor. Semiconductor Material and Device Characterization (3rd ed.). Hoboken, New Jersey, John Wiley & Sons, Inc. p 563-626.

Vinegoni, C, Cazzanelli M, Paveis L.2001. Porous silicon microcavities. In: Nalwa HS, editor. Silicon-based material and devices. San Diego, California, Academic Press. p 124-188.

_____

Arvin I. Mabilangan <arvinmabilangan@gmail.com>**, Niel Gabriel E. Saplagio, Eloise P. Anguluan, Neil Irvin F. Cabello, and Rhona Olivia M. Gonzales** are graduate students affiliated with the Condensed Matter Physics Laboratory of the National Institute of Physics, University of the Philippines Diliman.

Arnel A. Salvador, PhD <asalvadornip@gmail.com> is a Professor at the National Institute of Physics, University of the Philippines Diliman. Dr. Salvador earned his

bachelor's degree in Physics, *cum laude,* from the University of the Philippines Diliman. He earned his PhD in Physics from the University of Illinois at Urbana-Champaign in the United States.

Armando S. Somintac, PhD <somintac@gmail.com> is an Assistant Professor and currently the Program Coordinator of the Condensed Matter Physics Laboratory at the National Institute of Physics, University of the Philippines Diliman.